



Pediatric Imaging Pictorial Essay

Application of 7 tesla magnetic resonance imaging for pediatric neurological disorders: Early clinical experience

Kenichi Yamada¹, Junichi Yoshimura², Masaki Watanabe¹, Kiyotaka Suzuki¹

¹Center for Integrated Human Brain Science, ²Department of Neurosurgery, Brain Research Institute, Niigata University, Niigata, Japan.



***Corresponding author:**

Kenichi Yamada,
Center for Integrated Human
Brain Science, Brain Research
Institute, Niigata University,
Niigata, Japan; Hayakawa
Children's Clinic, Niigata, Japan.

kyamada@hachiicl.jp

Received : 29 September 2021
Accepted : 07 November 2021
Published : 02 December 2021

DOI
10.25259/JCIS_185_2021

Quick Response Code:



ABSTRACT

Ultra-high field magnetic resonance imaging (MRI) has been introduced for use in pediatric developmental neurology. While higher magnetic fields have certain advantages, optimized techniques with specific considerations are required to ensure rational and safe use in children and those with pediatric neurological disorders (PNDs). Here, we summarize our initial experience with clinical translational studies that utilized 7 tesla (T)-MRI in the fields of developmental neurology. T₂-reversed images and three-dimensional anisotropy contrast imaging enabled the depiction of targeted pathological brain structures with better spatial resolution. Diffusion imaging and susceptibility-weighted imaging enabled visualization of intracortical, subcortical, and intratumoral microstructures *in vivo* within highly limited scan times appropriate for patients with PNDs. 7T-MRI appears to have significant potential to enhance the depiction of the structural and functional properties of the brain, particularly those associated with atypical brain development.

Keywords: Three-dimensional anisotropy contrast, 7 Tesla, Brain development, Brain tumor, Prader-Willi syndrome

INTRODUCTION

Modern clinical developmental neurology has strived to achieve effective interventions that offer developmental support for patients with pediatric neurological disorders (PNDs). Magnetic resonance imaging (MRI) can non-invasively detect *in vivo* structural and functional alterations in the brain^[1,2] and could potentially help visualize detailed microstructural and functional properties, while maximizing physical and psychological safety. Here, we show our initial experiences of application of 7 tesla (T) MRI in developmental neurology to better contribute better understanding of human brain development and those in the brain of developmental neurological disorders.^[3]

SPECIFIC CONSIDERATION FOR USING 7T-MRI IN A PEDIATRIC STUDY

There are several basic characteristics of an ultra-high field MRI system that require specific consideration when studying pediatric participants. While the core elements do not differ in nature between studies in adults and children, the size, geometry, and development of children require more sophisticated optimizations of the system. As a detailed elaboration of each of these elements

This is an open-access article distributed under the terms of the Creative Commons Attribution-Non Commercial-Share Alike 4.0 License, which allows others to remix, tweak, and build upon the work non-commercially, as long as the author is credited and the new creations are licensed under the identical terms.

©2021 Published by Scientific Scholar on behalf of Journal of Clinical Imaging Science

is beyond the scope of this article, readers are referred to the following physics and engineering references.^[4-7]

Signal-to-noise ratio (SNR)

In MRI, the resonance frequency varies proportionally with the field strength. The higher the strength of the magnetic field, the better spectral resolution in magnetic resonance spectroscopy applications, and the higher the SNR:

$$SNR \propto B_0^{\frac{7}{4}}$$

Magnetic susceptibility effect

Paramagnetic susceptibility can be given according to the Brillouin equation:

$$\chi = \frac{\hbar\gamma}{2B_0} \tanh\left(\frac{\hbar\gamma B_0}{2kT}\right),$$

where γ is the gyromagnetic ratio, k is the Boltzmann constant, and T is the absolute temperature. The relationship between the magnetic susceptibility effect and field strength can be represented as follows:

$$\chi B_0 \sim \tanh(B_0).$$

The higher the field strength, the greater the magnetic susceptibility effect. While this is beneficial when enhancing the paramagnetic effect in imaging employing gradient-echo sequences (e.g., susceptibility-weighted imaging [SWI]), it may lead to imaging artifacts such as inhomogeneity in imaging employing spin-echo sequences.

Relaxation time

The Bloch equation is given as follows:

$$\frac{d}{dt}M(t) = \gamma M(t) \times B(t) - R\{M(t) - M_0\}$$

where R represents the relaxation matrix below:

$$R = \begin{pmatrix} 1/T2 & 0 & 0 \\ 0 & 1/T2 & 0 \\ 0 & 0 & 1/T1 \end{pmatrix}$$

With a higher magnetic field, the T1 signal increases in brain tissues, while the T2 signal independently decreases in gray matter, white matter, and CSF. For practical implementation of ultra-high field MRI in clinical developmental neuroscience, it is important to note that T1 contrast tends to be minimized, whereas T2 contrast tends to be emphasized.

Chemical shift

Chemical shift is a variation in resonance frequency due to variations in the electron distribution in each molecular structure. The degree of variation is proportional to the field strength, which is represented as follows:

$$\Delta\nu \sim \Delta B_0.$$

Accordingly, better spectral resolution can be achieved with a higher magnetic field strength in magnetic resonance spectroscopy applications. The details of this aspect fall outside the scope of this article.

Table 1: The imaging parameters for the images presented in this text.

	FOV (cm) Mat	Th (cm) Sp	TR (ms) TE	ETL FA (degree)	NEX/MPG b value	Scan time (min.)	Imaging option
7 Tesla							
FSE axial	18	3.0	5000	16	2 / -	4-5	ARC
	512	0	36.0	-	-		
(Focused image)	12	3.0	5000	16	2 / -	6-7	ARC
	512	0	36.0	-	-		
FLAIR axial	16	3.0	8000	1	1 / -	6-7	TI 1900
	256	0	129.3	-	-		
DWI axial	18	3.0	5000	16	2 / 25	6-7	ASSET
	256	0	82.4	-	2000, 1500, 1000		
(Focused image)	12	3.0	5000	16	3 / 25	6-7	
	128	0	90.1	-	2000, 1000		
SWI axial	8	5.0	220	-	4 / -	4-5	
	512	2.5	21.4	20	-		
3 Tesla							
FSE axial	200	5.0	6000	8	2 / -	3-4	ASSET
	512	2.5	25.7	-	-		

FOV: Field of view, Mat: Matrix, Th: Slice thickness, Sp: Interslice gap, TR: Repetition time, TE: Echo time, ETL: Echo train length, FA: Flip angle, NEX: Number of excitations, MPG: Motion probing gradient, FSE: Fast spin echo, FLAIR: Fluid-attenuated inversion recovery, DWI: Diffusion-weighted imaging, SWI: Susceptibility-weighted imaging, ARC: Autocalibrating reconstruction for cartesian imaging, TI: Inversion time, ASSET: Array spatial sensitivity encoding technique

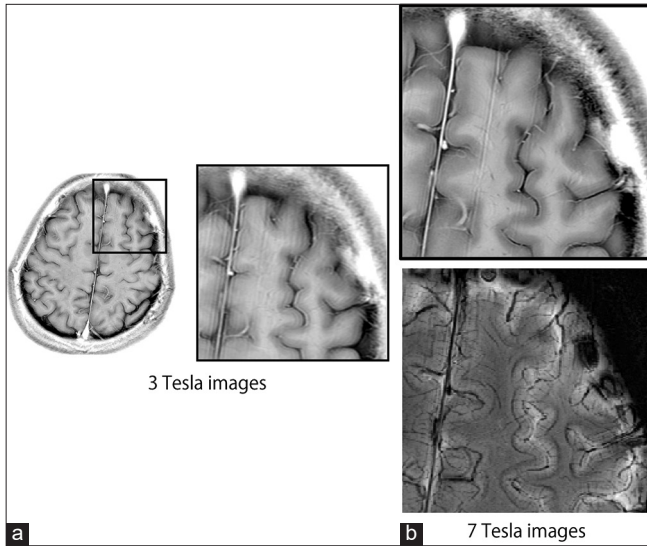


Figure 1: Comparative presentation of structural magnetic resonance images based on 3 Tesla (T) and 7T system. (a) An axial fast spin echo image and its zoomed presentation in the left frontal area based on 3T system. The resolution is field of view (FOV) 200 mm/512 pixel = 0.39 mm/pixel. The scan time is about 5 min. (b) An axial fast spin echo image and susceptibility-weighted image in the same slice based on 7T system. The resolution is FOV 80 mm/512 pixel = 0.16 mm/pixel. The imaging time is about 4 min. The detail of the imaging parameters are shown in Table 1.

PREPARATION AND IMAGING PROCEDURES

Preparation

We introduced a simulation protocol with a mock scanner for preparation as a systematic approach for pediatric 7T-MRI without sedation. Before actual imaging, an original preparation protocol involving the “zero-tesla” mock scanner system was developed in-house and applied to these participants. The participants were permitted to watch their favorite movies with audiovisual aids while lying inside the mock scanner. This strategy avoids the need to administer any sedative agent to all the participants.^[8-10]

Imaging procedures

A 7T-MRI system (MR950, General Electric, Waukesha, WI, USA) with a 900-mm, clear-bore, superconducting magnet and a 32-channel and NOVA phased-array head coil was used for all imaging studies. Safety of the participants was most prioritized to maximize physical and psychological safety. The specific absorptive ratio was maintained to be controlled below the safety level during the scan. The total actual imaging time per study was limited within about 30-40 min. Earplugs and soft cushions insulating the head and neck were used by all participants to reduce sensory discomfort.

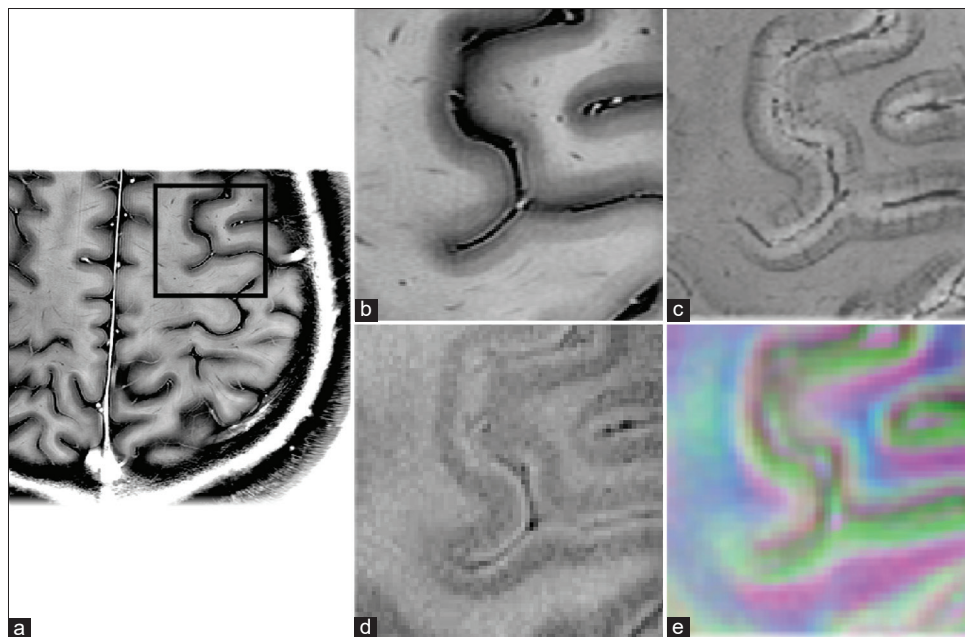


Figure 2: High-resolution 7T magnetic resonance images in an adult individual with typical development (TD). (a) T2-reversed image. The rectangular line corresponds with the field-of-view in (b-e). (b) Magnified image, (c) susceptibility-weighted image, (d) fluid-attenuated inversion-recovery image based on T₂-contrast image. (e) 3-dimensional anisotropy contrast image. While the detailed information on white and gray matter structures is shown, a wide range of intracortical microstructural properties can be visualized using a series of contrast images obtained with the 7T system.

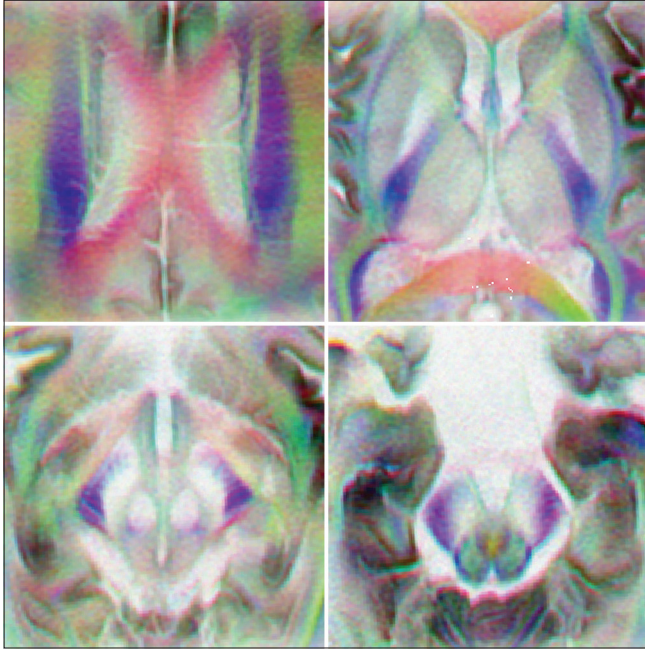


Figure 3: Three-dimensional anisotropy contrast (3DAC) images in an adult participant with TD. 3DAC imaging is characterized by a combination of a vector contrast with a higher signal-to-noise ratio, leading to more detailed anatomical resolution and subsequent identification of neural pathways and nuclei.

During image acquisition, participants enjoyed watching their favorite movies, which were presented using an eyeglass device and headphones. As a result, studies were successfully completed, resulting in acceptable image quality. The imaging parameters in the figures shown below were summarized in Table 1, together with the those using 3T images. The detailed procedures for reconstructing images are encouraged to see the reference paper for interested readers.

Focus on *in vivo* microstructural imaging analysis of human brain development

Even in modern clinical neuroimaging practice, where functional imaging analysis is predominant, the acquisition of detailed structural images remains important as the first step for accurate lesion localization and pathological identification. Representative examples are described in the following sections and basic characteristics of higher-field systems are summarized in Supplement.

High-resolution structural imaging

T₂-weighted imaging (T2WI) is sensitive to the detection of pathological and developmental changes. T₂-reversed imaging (T2R) is based on the concept of improving

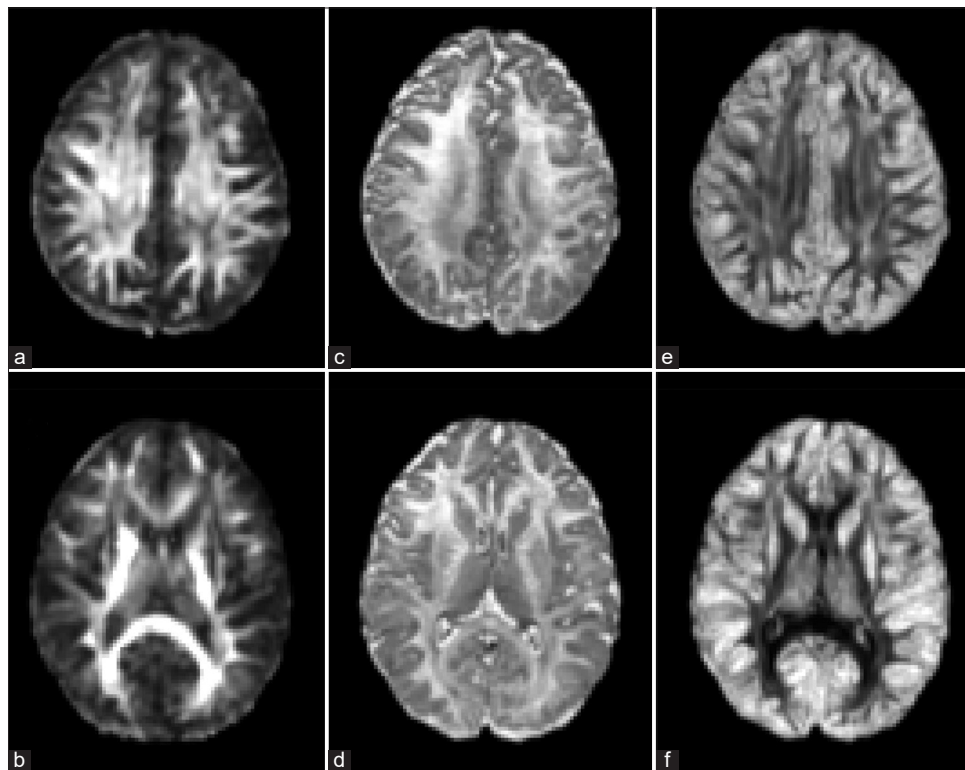


Figure 4: Representative index maps reflecting diffusion characteristics from an adult individual with TD. Fractional anisotropy maps (a and b), neural density index maps (c and d), and orientation dispersion index maps (e and f) calculated based on neurite orientation dispersion and density imaging. Data were obtained in an adult participant with TD.

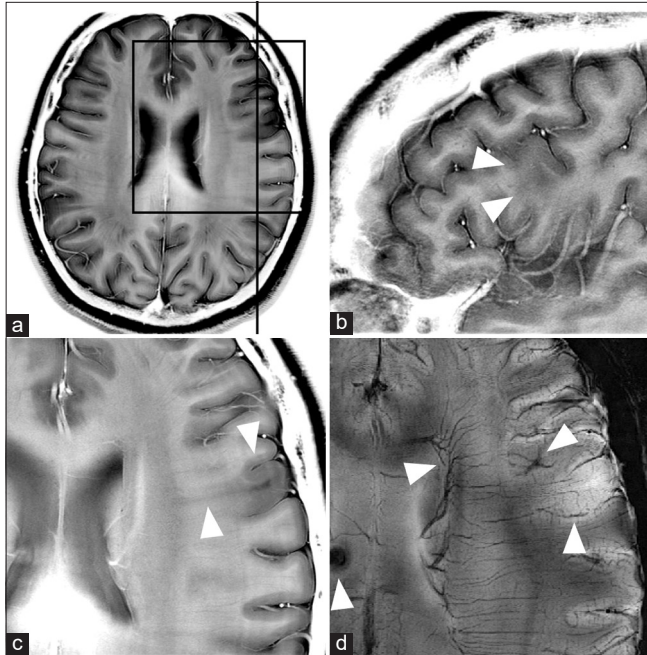


Figure 5: Focused structural images in a patient with tuberous sclerosis complex. (a) Axial image showing cortical tubers over the right frontal areas. (b) Sagittal image of the tubers. (c) Focused structural image of the lesions, indicating intratuberal structure and low signal intensity between the tuber and third ventricle as a “transmantle sign.” (d) Susceptibility-weighted image. The structural distribution of the perituberal microvasculature can be visualized. Moreover, enhancement of a periventricular nodule with low signal intensity due to increased susceptibility associated with its tissue properties can be observed in the left third ventricle.

perceptual resolution by reversing the grayscale of T2WI, which expands finer contrast resolutions by taking full advantage of the higher signal-to-noise ratio afforded by an ultra-high field system [Figure 1].^[11,12] In higher magnetic fields, moreover, enhanced susceptibility contrast provides the opportunity to improve the visualization of the brain microstructure and microvascular flow, as each element such as trace metals and/or myelin has *in vivo* unique susceptibility. Moreover, while subtle changes associated with reduced microvascular flow in intracortical structures can be detectable with susceptibility-weighted imaging (SWI), which has been shown to correlate with age,^[13,14] extrapolating these findings to childhood has demonstrated the contribution of the myelination process and layer-specific variations in iron content to the susceptibility signal source.^[15,16]

Functional property imaging

While the fluid-attenuated inversion recovery (FLAIR) sequence with T₂ weighting is commonly used to suppress high signal intensity arising from cerebrospinal fluid (CSF), such as that from unrestricted water, it unexpectedly detects high-intensity signals in a thin layer of the normal cortex, referred to as the “FLAIR hyperintense rim (FHR).” A recent investigation that employed a 7T system demonstrated that the structure that gives rise to the FHR has a unique combination of intrinsic contrast parameters: Low proton density, long T₂, and disproportionately short T₁. These characteristics reflect the structural and functional properties of the glia limitans externa, which are highly dependent on

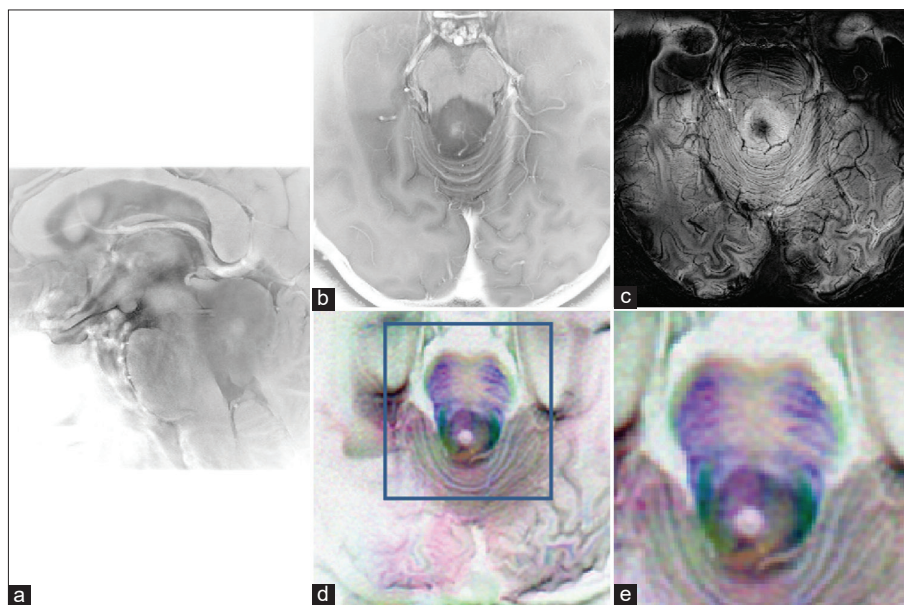


Figure 6: Representative images of a brain tumor in a 21-year-old woman. (a) Sagittal image showing a tumor mass with a central vascular supply in a tectal lesion. (b) Midline axial image showing the lesion expanding into the midbrain structures. (c) Susceptibility-weighted imaging provides information regarding the venous contribution in intra- and peritumoral structures. (d) 3DAC imaging showing the detailed anatomical relationship between the tumor mass and neural pathways in the midbrain. (e) Magnified 3DAC image and the image in the same axial slice as in (d).

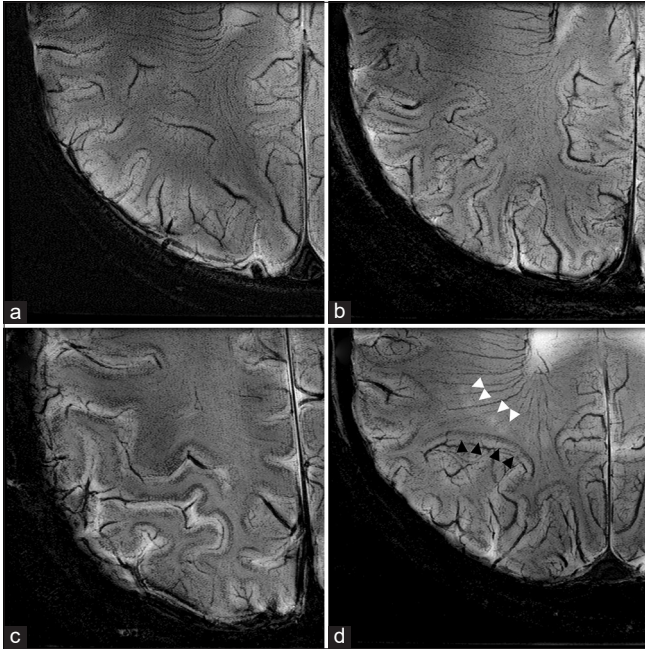


Figure 7: Susceptibility-weighted images obtained from participants with TD and an individual with a neurodevelopmental disorder. (a) A 10-year-old boy with TD, (b) a 20-year-old woman with TD, (c) a 39-year-old woman with TD, (d) a 36-year-old woman with Down syndrome. When compared to participants with TD, the patient with Down syndrome exhibited high-intensity lesions in the deep white matter, which did not appear to be centralized with the deep medullary vein, indicating that these lesions were not likely to be those observed in patients with multiple sclerosis but rather indicative of microangiopathy (white arrowhead). However, the intracortical high-susceptibility region-corticomedullary junction exhibits age-related enhancement, indicating a potential for the assessment of cortical functionality-associated flow (black arrowhead).

the physiological functionality of the aquaporin [Figure 2].^[17]

The advantages of a higher magnetic field are reflected in better image resolution, with a narrow field of view, due to a better signal-to-noise ratio. Diffusion-weighted imaging (DWI) makes it possible to obtain more detailed microstructural information.^[18] 3-dimensional anisotropy contrast (3DAC) imaging is characterized by a combination of a vector contrast with a higher signal-to-noise ratio,^[19,20] providing more detailed anatomical resolution and subsequently allowing the identification of neural pathways [Figure 3]. Due to a shorter scan time that is beneficial for pediatric participants, subcortical and intracortical maturational alterations were clearly visualized using DWI. A full spectrum of information on anatomical and functional properties on the same slice, which are obtainable using various indices based on advanced diffusion imaging, e.g. neurite orientation dispersion and density imaging, are shown in Figure 4.

Given that it is still under development and far from a clinical application on the 7T system, spectroscopic (chemical shift)

imaging is beyond the scope of the current essay, if fruitful for assessing maturational alteration of the developing brain in childhood.^[21]

CLINICAL IMAGING USING A 7T MRI FOR DEVELOPMENTAL NEUROLOGICAL DISORDERS

Here, we reviewed 7T serial MR images obtained from healthy volunteers and individuals with PNDs. The study was conducted in accordance with the human research guidelines of the Institutional Review Board and approved by the appropriate Research Ethics Committee (approval no. 2482). Written informed consent was obtained from all participants or their parents or guardians if necessary, and the study was conducted in accordance with the Declaration of Helsinki.

Neurocutaneous syndrome accompanied by brain malformation

Brain malformation in individuals with PNDs require better understanding and management based on pathophysiology of the brain. Accurate and detailed information about the lesion can provide a better treatment strategy for epilepsy and appropriate support associated with functional localization. A representative case of neurocutaneous syndrome with epilepsy in a patient with tuberous sclerosis complex is presented in Figure 5.

Pediatric brain tumor

The 7T system allows for a more focused analysis of tumor tissue characteristics and the environment surrounding the mass, including vascular supply, calcification, and CSF outlets. T₂R imaging, supported by 3DAC imaging, can reveal finer microanatomical abnormalities in patients with hypothalamic, pituitary, and midbrain tectal lesions, such as compressed neural pathways. SWI enhances microvascular structures and shows their distribution around the tumor mass in brainstem lesions [Figure 6]. In particular, the ability to estimate the histological type and firmness of the tumor preoperatively is advantageous given that rigidity and susceptibility to bleeding play a major role in evaluating the difficulty of tumor removal.

Specific behavioral characteristics associated with genetic syndrome and childhood adverse experience

Neuropathological analyzes have revealed that several genetic syndromes, for example, Down syndrome (DS), exhibit microangiopathy associated with amyloid deposition;^[22,23] however, possible susceptibility to dementia remains fully revealed *in vivo*. Early 7T-SWI studies have demonstrated that the cortico-medullary junction-high susceptibility region

(CMJ-HSR) was enhanced in older adults and patients with dementia.^[13,17] We have applied SWI CMJ-HSR and have detected alterations in an individual with DS, which might be related to cortical neuropathophysiological alterations [Figure 7]. Considering the microstructural alterations detected in the white matter in individuals with Prader-Willi syndrome and those exposed to childhood maltreatment using 3T-MRI,^[2,24-28] 7T-SWI studies may reveal cortical microstructural alterations in individuals with congenital genetic syndrome and those with early adverse experiences.

CONCLUSION

7T-MRI appears to have significant potential to enhance the depiction of the structural and functional properties of the brain, particularly those associated with typical and atypical brain development. A thorough understanding of the benefits and limitations of ultra-high field systems, along with attempts to maximize physical and psychological safety for patients, would facilitate the evaluation of the pathophysiology of PNDs.

Acknowledgments

We thank and pay tribute to Tsutomu Nakada, MD, PhD, FAAN, Emeritus Professor and Director, Center for Integrated Human Brain Science, Brain Research Institute, University of Niigata.

Authors' contributions

Kenichi Yamada (KY): Study conception and design; acquisition of data; analysis and interpretation of data; drafting of manuscript. Junichi Yoshimura (JY): acquisition of data; analysis and interpretation of data; drafting of manuscript. Masaki Watanabe (MW): Acquisition of data; critical revision. Kiyotaka Suzuki (KS): Acquisition of data; analysis and interpretation of data; critical revision. All authors read and approved the final manuscript.

Compliance with ethical standards

The study was conducted in accordance with the human research guidelines of the Institutional Review Board and approved by the appropriate Research Ethics Committee (approval number #2482). Written informed consent was obtained from all participants or their parents or guardians if necessary, and the study was conducted in accordance with the Declaration of Helsinki.

Declaration of patient consent

The authors certify that they have obtained all appropriate patient consent.

Financial support and sponsorship

This study was supported by KAKENHI grants from the Japanese Society of Promotion of Science (grant number 17K10049 to Kenichi Yamada). The funding source had no involvement in the study design; in the collection, analysis, and interpretation of data; in the writing of the report; or in the decision to submit the article for publication.

Conflicts of interest

There are no conflicts of interest.

REFERENCES

1. Suzuki Y, Matsuzawa H, Kwee IL, Nakada T. Absolute eigenvalue diffusion tensor analysis for human brain maturation. *NMR Biomed* 2003;16:257-60.
2. Yamada K, Matsuzawa H, Uchiyama M, Kwee IL, Nakada T. Brain developmental abnormalities in Prader-Willi syndrome detected by diffusion tensor imaging. *Pediatrics* 2006;118:e442-8.
3. Nakada T. Clinical application of high and ultra high-field MRI. *Brain Dev* 2007;29:325-35.
4. Brown RW, Cheong YCN, Haacke EM, Thompson MR, Venkatesan R. *Magnetic Resonance Imaging: Physical Principles and Sequence Design*. 2nd ed. Hoboken, New Jersey: Wiley-Blackwell; 2014.
5. Robitaille PM, Berliner L. *Ultra-High Field Magnetic Resonance Imaging*. New York: Springer Science and Business Media, LLC; 2006.
6. Nakada T, Matsuzawa H, Suzuki K. *Magnetic Resonance Imaging*. Tokyo: Japan Medical Journal; 2012.
7. Nakada T, Houkin K. *MRA of Brain and Spinal Cord*. Tokyo: Chugai-Igakusya; 1997.
8. Japan Pediatric Society, Japanese Society of Pediatric Anesthesiology, Japanese Society of Pediatric Radiology Recommendations on Pediatric Sedation for MR Examinations 2015; 2015.
9. Coté CJ, Wilson S, American Academy of Pediatrics, American Academy of Pediatric Dentistry. Guidelines for monitoring and management of pediatric patients before, during, and after sedation for diagnostic and therapeutic procedures. *Pediatrics* 2016;138:e20161212.
10. Yamada K, Suzuki Y, Ueki S, Itoh K, Watanabe M, Suzuki K, *et al.* Participant-driven simulation protocol with a mock scanner for pediatric magnetic resonance neuroimaging preparation without sedation. *Clin Simul Nurs* 2020;47:40-7.
11. Fujii Y, Nakayama N, Nakada T. High-resolution T2-reversed magnetic resonance imaging on a high magnetic field system. Technical note. *J Neurosurg* 1998;89:492-5.
12. Nakada T, Kwee IL, Fujii Y, Knight RT. High-field, T2 reversed MRI of the hippocampus in transient global amnesia. *Neurology* 2005;64:1170-4.
13. Nakada T, Matsuzawa H, Igarashi H, Fujii Y, Kwee IL. *In vivo* visualization of senile-plaque-like pathology in Alzheimer's disease patients by MR microscopy on a 7T system. *J Neuroimaging* 2008;18:125-9.
14. Nakada T, Matsuzawa H, Igarashi H, Kwee IL. Expansion of

- corticomedullary junction high-susceptibility region (CMJ-HSR) with aging: A clue in the pathogenesis of Alzheimer's disease? *J Neuroimaging* 2012;22:379-83.
15. Glasser MF, Goyal MS, Preuss TM, Raichle ME, van Essen DC. Trends and properties of human cerebral cortex: Correlations with cortical myelin content. *Neuroimage* 2014;93:165-75.
 16. Fukunaga M, Li TQ, van Gelderen P, de Zwart JA, Shmueli K, Yao B, *et al.* Layer-specific variation of iron content in cerebral cortex as a source of MRI contrast. *Proc Natl Acad Sci USA* 2010;107:3834-39.
 17. Suzuki K, Yamada K, Nakada K, Suzuki Y, Watanabe M, Kwee IL, *et al.* MRI characteristics of the glia limitans externa: A 7T study. *Magn Reson Imaging* 2017;44:140-5.
 18. Zhang H, Schneider T, Wheeler-Kingshott CA, Alexander DC. NODDI: Practical *in vivo* neurite orientation dispersion and density imaging of the human brain. *Neuroimage* 2012;61:1000-16.
 19. Nakada T, Nakayama N, Fujii Y, Kwee IL. Clinical application of three-dimensional anisotropy contrast magnetic resonance axonography. Technical note. *J Neurosurg* 1999;90:791-5.
 20. Nakada T, Matsuzawa H, Fujii Y, Takahashi H, Nishizawa M, Kwee IL. Three-dimensional anisotropy contrast periodically rotated overlapping parallel lines with enhanced reconstruction (3DAC PROPELLER) on a 3.0T system: A new modality for routine clinical neuroimaging. *J Neuroimaging* 2006;16:206-11.
 21. Shimizu M, Suzuki Y, Yamada K, Ueki S, Watanabe M, Igarashi H, *et al.* Maturation decrease of glutamate in the human cerebral cortex from childhood to young adulthood: A ¹H-MR spectroscopy study. *Pediatr Res* 2017;82:749-52.
 22. Carmona-Iragui M, Videla L, Lleó A, Fortea J. Down syndrome, Alzheimer disease, and cerebral amyloid angiopathy: The complex triangle of brain amyloidosis. *Dev Neurobiol* 2019;79:716-37.
 23. Yanai K, Ishida Y, Nishido H, Miyamoto S, Yamazaki K, Hoya K. Multiple cerebral hemorrhagic lesions depicted by susceptibility-weighted imaging in a patient with down syndrome: Case report. *J Stroke Cerebrovasc Dis* 2019;28:e37-8.
 24. Rice LJ, Lagopoulos J, Brammer M, Einfeld SL. Microstructural white matter tract alteration in Prader-Willi syndrome: A diffusion tensor imaging study. *Am J Med Genet C Semin Med Genet* 2017;175:362-7.
 25. Lukoshe A, White T, Schmidt MN, van der Lugt A, Hokken-Koelega AC. Divergent structural brain abnormalities between different genetic subtypes of children with Prader-Willi syndrome. *J Neurodev Disord* 2013;5:31.
 26. Yamada K, Watanabe M, Suzuki K, Suzuki Y. Cerebellar volumes associate with behavioral phenotypes in Prader-Willi syndrome. *Cerebellum* 2020;19:778-87.
 27. Yamada K, Suzuki K, Watanabe M. Altered functional network architecture of the brain in Prader-Willi syndrome. *Brain Connect* 2021;Jun 29. Doi:10.1089/brain.2020.0914. Online ahead of print.
 28. Yamada K, Suzuki Y, Okuyama M, Watanabe M, Nakada T. Developmental abnormalities of the brain exposed to childhood maltreatment detected by diffusion tensor imaging. *Neurol Res* 2019;41:19-25.

How to cite this article: Yamada K, Yoshimura J, Watanabe M, Suzuki K. Application of 7 tesla magnetic resonance imaging for pediatric neurological disorders: Early clinical experience. *J Clin Imaging Sci* 2021;11:65.